Parachute-Suspended Solar Pointing Control System

George T. Sakoda,* Robert J. Fujimoto,* and John M. Shigemoto†
Lockheed Missiles and Space Company, Inc., Sunnyvale, California
and
Richard M. Windsor‡
NASA Goddard Space Flight Center, Greenbelt, Maryland

A high-altitude, parachute-suspended solar pointing control system has been developed and flight tested for use in the altitude range 30 to 70 km. This development provides an opportunity for extended solar observations at altitudes higher than that attainable by helium balloons. The new system utilizes the NASA high-altitude cross parachute to slow the descent of a rocket-launched payload allowing observations in the region of interest. Solar pointing is established by using solar sensors in conjunction with a servo controlled platform and cold gas thrusters for payload roll control. The inherent spin of the cross parachute is decoupled by a swivel joint attached to the parachute suspension lines. This paper describes the design, test, and flight performance of the new system which was successfully launched on NASA Rocket 30.006GU on Sept. 15, 1980.

Introduction

THE development of the parachute-suspended solar pointing control system resulted from a NASA requirement to extend measurements of the Earth's ozone layer to the altitude region 30 to 70 km. A solar pointing system is required since the ozone profile is established by recording the atmospheric absorption of the solar irradiance. Previous experiments on helium balloons were limited to a maximum altitude of 40 km. Solar pointed sounding rockets transverse the desired altitude range but are unsuitable because of the rapid descent at atmospheric drag forces which limit pointing accuracy. Currently, the practical limit for low-altitude rocket pointing control is approximately 65 km. Therefore, it was clear that a new system configuration would be required to provide a stabilized solar pointed platform in the desired altitude region.

The configuration established by NASA utilizes an Orion sounding rocket boost vehicle and a high-altitude parachute to slow the descent of the payload. This combination was successfully launched with an uncontrolled payload on July 14, 1977, NASA Rocket 12.027GT.[1]

To meet the solar pointing requirements, a system based on the highly successful Solar Pointing Attitude Rocket Control Systems (SPARCS) was developed by NASA and the Lockheed SPARCS Project.[2,3]

System Configuration and Flight Sequence

The vehicle configuration illustrated in Fig. 1 consists of an Orion sounding rocket as the boost vehicle, a high-altitude parachute, and a payload section.

The Orion rocket is ideally suited to place a small payload in a convenient trajectory to achieve the desired altitude. Near apogee, the payload is separated from the motor, exposing the experiment section to the atmosphere. Following separation the payload is despun with a yo-yo and the nose cone is ejected. Upon ejection, the nose cone mechanically extracts the parachute assuring proper deployment in the low-atmosphere environment.

After deployment, the canopy is inflated and solar acquisition is established. The low-velocity parachute slows the payload descent such that the transition through the desired altitude range of 60 to 30 km is approximately 500. Figure 2 illustrates the sequence of events for a solar pointing mission.

Parachute and Payload Motions

The nylon parachute is a 63.5-ft-diam cross design with a panel of 17 ft. There are a total of 28 suspension lines 63.5 ft long, constructed of 100-lb test nylon. The test flight revealed a multimodal motion of the suspended payload. First, the parachute had an initial spin rate of 30 rpm which decreased to about 1 rpm at lower altitudes. Second, a pendulous coning motion developed. The amplitude of the coning motion rapidly settled down from a near-horizontal spin to about 15 deg (half-angle), 17 s after canopy inflation. The frequency of this motion was 0.2 Hz with an amplitude decreasing with altitude, as shown in Fig. 3. Third, a vibrating mode 1.5 Hz oscillation occurred with an initial half-angle amplitude of 1 deg which increased to about 10 deg with decreasing altitude. This disturbance appears to be initiated by the vibration of the parachute suspension lines due to high-altitude winds. The two oscillatory motions of the parachute/payload system can be modeled by a double pendulum using the swivel as the connecting link. Figure 4 illustrates the parachute-suspended payload motion.

The inherent spin motion of the parachute is decoupled from the payload by a swivel joint between the parachute suspension lines and the payload. The swivel consists of two radial bearings and a thrust which supports the weight of the payload.

Control System

The solar pointing control system consists of a gimbaled pitch servo platform and a cold gas thrust system for roll control. Yaw control is not provided since angular motion about the solar vector is acceptable in terms of the experiment operation. Pointing information is provided by coarse solar sensors mounted on the circumference of the payload support

Presented as Paper 82-1733 at the AIAA 6th Sounding Rocket Conference, Orlando, Fla., Oct. 26-28, 1982; submitted Nov. 3, 1982; revision received April 21, 1983. Copyright © American Institute of Aeronautics and Astronautics, Inc., 1982. All rights reserved.

*Research Specialist, SPARCS Project.
†Manager, SPARCS Project.
‡Program Manager, SPARCS.

package and a fine pointing sensor on the gimbaled platform. Figure 5 illustrates the major components of the control system.

Coarse solar acquisition is initiated after deployment of the parachute using the coarse solar sensors. The sensors, in conjunction with the cold gas thrusters, rotate the payload about the longitudinal (roll) axis until the spectrometer and fine-pointing sensor face the sun. The gimbaled platform is preprogrammed with a bias such that the spectrometer is coarsely aligned with the solar vector when the payload viewing port faces the sun. A sun presence detector mounted adjacent to the spectrometer detects the sun and switches pointing control to the fine-pointing sensor and initiates the controller fine-pointing mode of operation. At this time, the pitch servoloop is activated and the gimbal platform is driven until the pointing sensor is nulled. Damping is provided by a three-axis rate gyro.

A pneumatic cold gas thruster system provides angular rotation about the payload roll axis. A 7-in. spherical gas storage tank dictated by availablity and size constraints limited the storage propellant.

SPARCS solar sensors (Fig. 6) are used to provide pointing error signals to the controller. The fine-pointing sensor mounted on the experiment housing is the Miniature Acquisition Sun Sensor (MASS). This sensor provides two-axis pointing error signals and has a ± 40 deg field of v iew. The sun presence sensor mounted adjacent to the MASS provides a mode switching signal when the sun is within ± 20 deg of the pointing axis. This signal which is used to switch the controller from coarse acquisition to fine pointing.

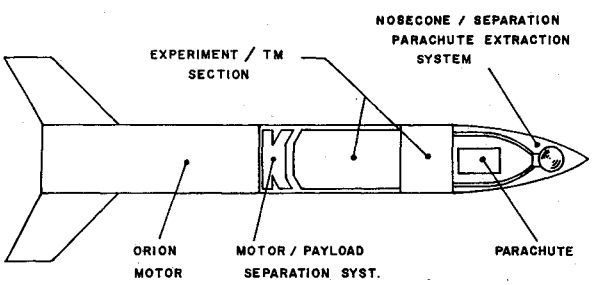

Fig. 1 Vehicle configuration.

Three coarse solar sensors are mounted on the circumference of the payload, Fig. 5. Two of the sensors are 180 deg apart and develop an error signal which is used in conjunction with the MASS signal to enable the gas jets. The third sensor location midway between the two sensors is shadowed when the playload is facing the sun. It has a field of view of 15 deg and serves to detect the unstable null position, thus aiding in rapid solar acquisition.

The fine-pointing sensor (MASS) provides two-axis pointing error signals which can be defined in terms of payload motion. The sensor outputs are as follows:

$\psi_B \sin\lambda - \phi_B \cos\lambda$ = roll sensor

$\lambda - \epsilon + \theta_B$ = pitch sensor

λ = sun angle relative to a plane tangent to the Earth's surface

ψ_B = body yaw motion (rotation about J_B axis)

ϕ_B = body roll motion (rotation about K_B axis)

θ_B = body pitch motion (rotation about I_B axis)

ϵ = gimbal platform elevation angle relative to the body axis J_B

The payload and gimbal reference frames are defined by right-hand orthogonal unit vectors as illustrated in Fig. 7. K_B is aligned with the longitudinal axis and is pointed upward toward the parachute. In the controlled mode, the platform axis J_P is aligned with the solar vector.

The coarse solar sensors (CSS) mounted on the body frame detect motion of the I_B body axis relative to the solar vector. The sensor output for small angles can be expressed as follows:

$$\psi_B \sin(\lambda\text{-}\theta) - \phi_B \cos(\lambda\text{-}\theta) = \text{CSS}$$

A restriction on the control loop was dictated by the available control thrust from the gas jets. The control jet force level of 0.24 lb. was a compromise between operating time and pointing error. With a moment arm of 15 in. and maximum control force (2 jets) of 0.48 lb, the maximum control acceleration is 68.83 deg/s^2. This level is not sufficient to control the 1.5 Hz disturbance but is acceptable for controlling the 0.2 Hz disturbance frequency. This fact was

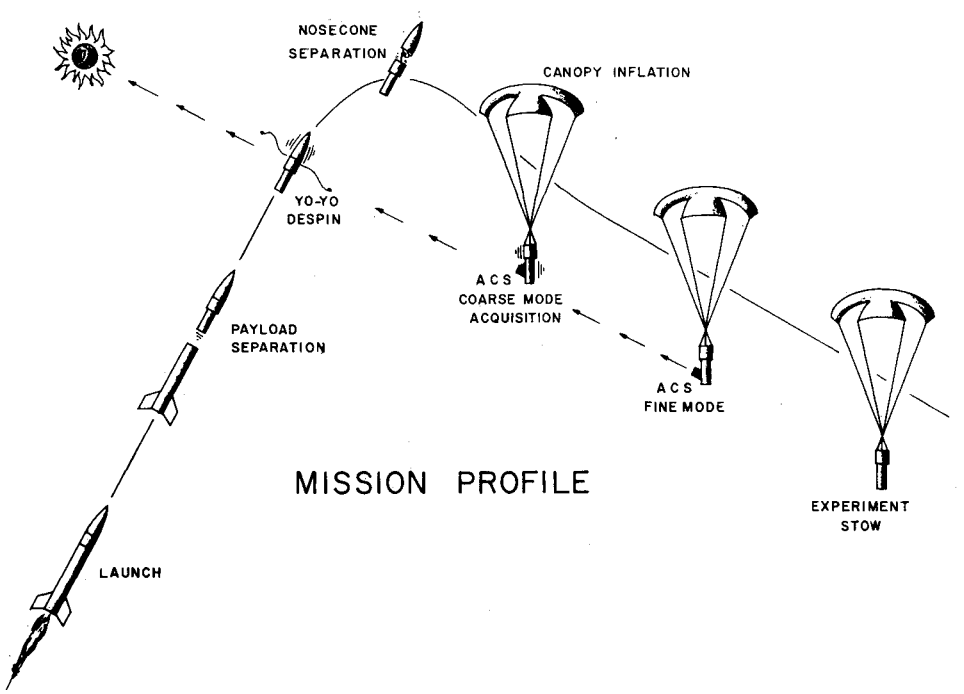

Fig. 2 Mission profile.

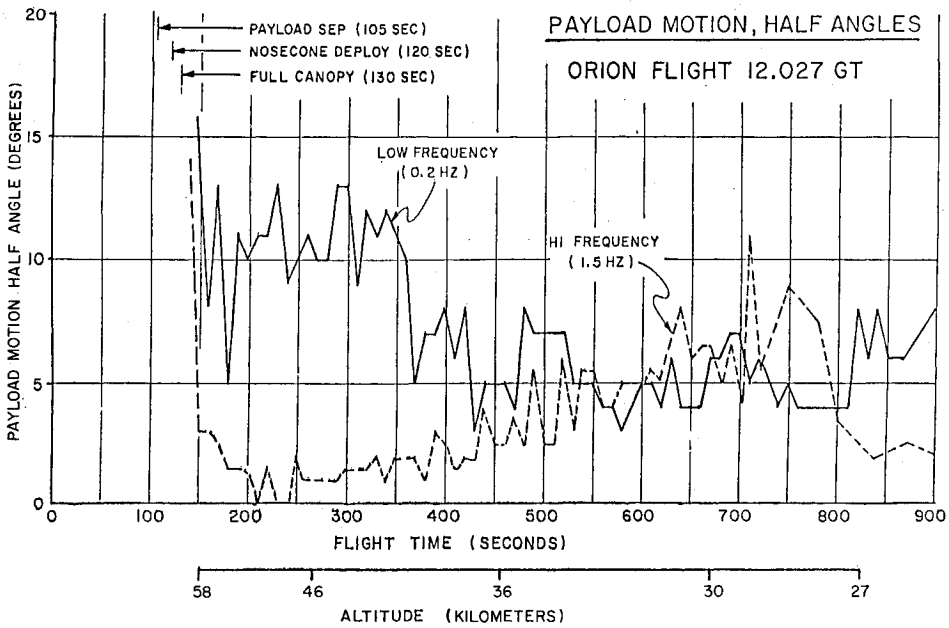

Fig. 3 Payload motion, half-angles.

known prior to selection of the thrust force level but was deemed acceptable since the amplitude of the 1.5 Hz disturbance was within the pointing error requirements (excursions up to ± 7 deg permissible).

With the available control acceleration of 68.83 deg/s^2, the maximum disturbance amplitude at 1.5 Hz which can be corrected is 0.775 deg. It is evident that without correction, the 1.5 Hz disturbance level would saturate the control electronics. For this reason, a 1.5 Hz notch filter was incorporated in the sensor and gyro compensation circuitry.

Pitch

The pitch servo loop response is sufficient to correct the predicted payload disturbances, therefore the 1.5 Hz notch filter is not required in this loop.

The servo system is comprised of a dc gear motor coupled to the experiment gimbal shaft by a pulley and belt arrangement. Test data disclosed a 10 Hz resonance caused by the flexibility of the pulley belt. This undesirable motion introduced a 10 Hz error signal in the pitch servo electronics. A 10 Hz notch filter was incorporated in the electronics to minimize the effects of the mechanical resonance. Figure 8 illustrates a simplified block diagram of the pitch control loop. The loop has a grain margin of 24 dB, a phase margin of -70 deg, and a closed loop bandwidth of 4.8 Hz.

Roll

The roll servo loop consists of a two-axis, body-mounted rate gyro and a solar sensor, detecting motion of the I_B body axis relative to the solar vector. In the coarse acquisition mode the CSS is used as the pointing sensor. After sun presence is detected in the front viewing port, the controller switches to the fine-pointing sensor (MASS).

The payload coning motion induced by parachute disturbances exceeds 15 deg. Looking at the components of the sensor output, it is evident that a large roll body motion is required to keep the CSS and the fine-pointing roll sensor outputs at zero. The roll body motion required to offset the yaw motion is

$$\theta_B = \psi_B \tan \lambda$$

For a payload coning motion of 15 deg and a sun angle λ of 60 deg, roll body correction of 26 deg will be required. Since the tangent term increases rapidly above 60 deg, the launch time

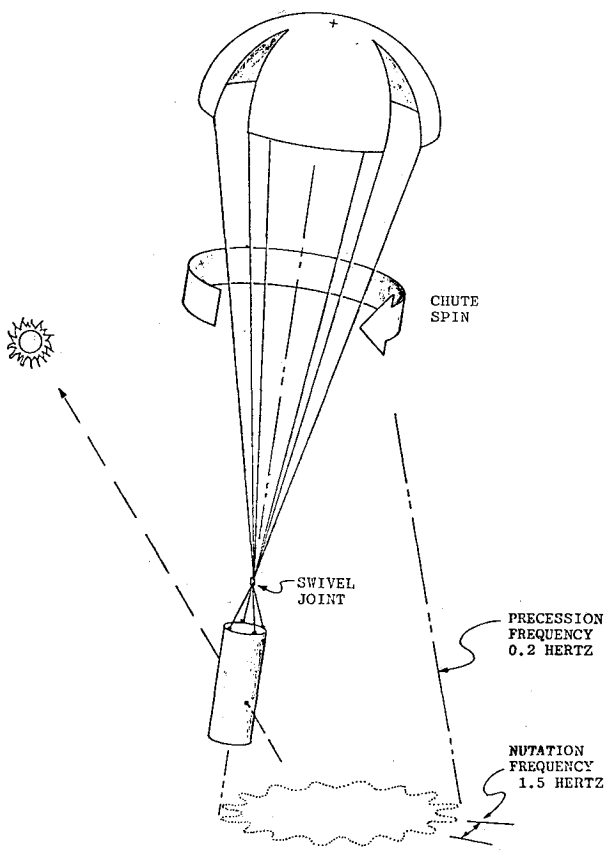

Fig. 4 Payload moton.

was restricted to periods where the sun angle is less than 55 deg. This assures that the roll motion will be within controllable limits.

The roll controller configuration can be derived from the basic control system shown in Fig. 9.

The block diagram illustrates the contribution of the large yaw disturbance to the system error.

From Fig. 9,

$$E(S) = \psi_B \sin \lambda - \phi_B \cos \lambda$$

$$\phi_B = \mathrm{E(S)K_A}\left(\frac{H_I}{S^2 + K_I K_g S}\right)$$

solving for $E(S)$,

$$E(S) = \frac{\psi_B \sin\lambda (S^2 + K_I K_g S)}{S^2 + K^{II} K_g S + K_A K_I \cos\lambda}$$

The earlier discussion showed that ψ_B is significant due to the parachute coning motion. To eliminate the ψ_B contribution to the system error, a correction term of the form $\psi_B S\ (J_A S + K_B)$ must be introduced. This term was implemented by using a yaw rate gyro as shown in the final configuration (Fig. 10). The term was scaled to cancel the ψ_B contribution previously shown in $E(S)$. In the solution of the closed-loop equations, it will be found that the gain terms (K_A, K_B) contain a "tanλ" term. Since the sun angle λ is shown prior to launch, this term may be implemented as a fixed gain.

Ground Test

Testing of the control system was accomplished by simulating the parachute disturbances. A crane was used to suspend the payload with a cable simulating the suspension lines. Attachment to the payload was made using the flight payload harness and swivel joint. This arrangement closely duplicated the expected flight disturbance profile when manually excited by test personnel. It was determined during the test that the damping factor and frequency of the nominal 1.5 Hz disturbance was a function of the harness arrangement and line length from the payload to the swivel. An optimum configuration in terms of controller performance was experimentally determined and incorporated for the actual flight.

The 0.2 Hz coning motion experienced in flight was induced by swinging the payload in a conical motion. Performance in this mode of operation was easily simulated, but the 1.5 Hz disturbance was difficult since the oscillation was only achieved by repeatedly disturbing the payload with a tie line. The final ground test data performed prior to launch at White Sands Missile Range (WSMR) demonstrated that the system would meet the mission requirements. Pitch error was less

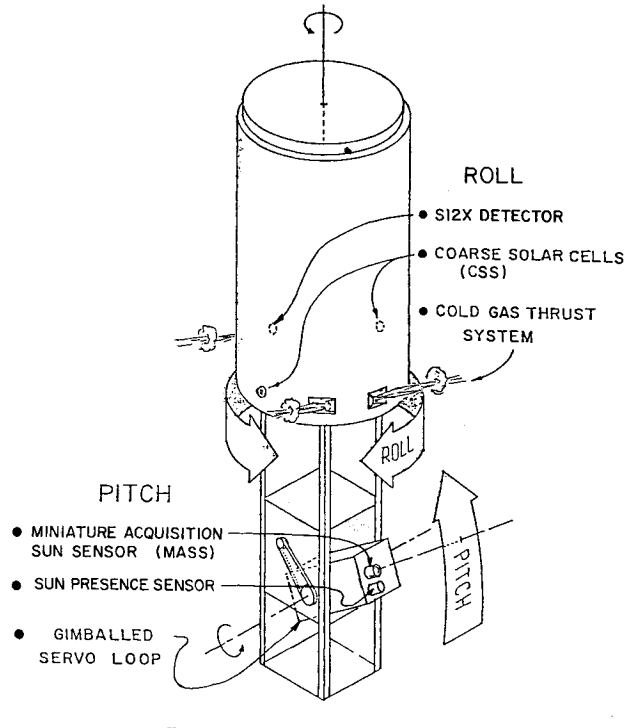

Fig. 5 Control system configuration.

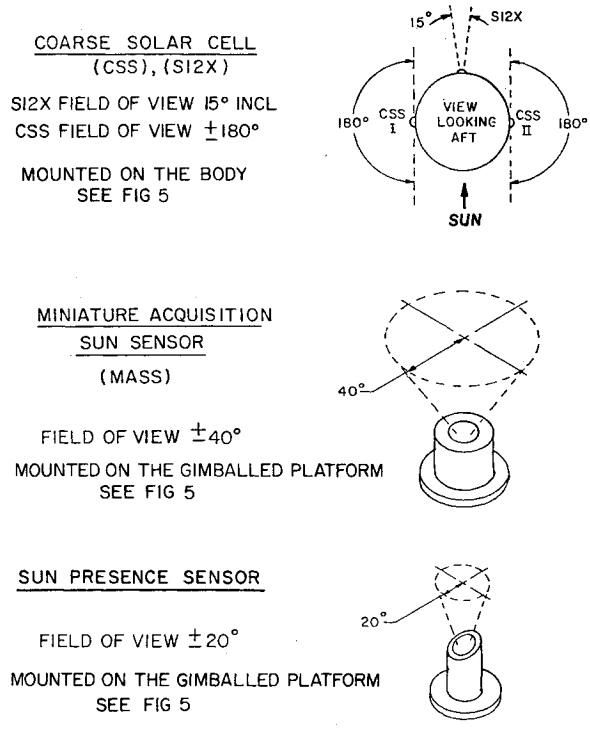

Fig. 6 Solar sensors.

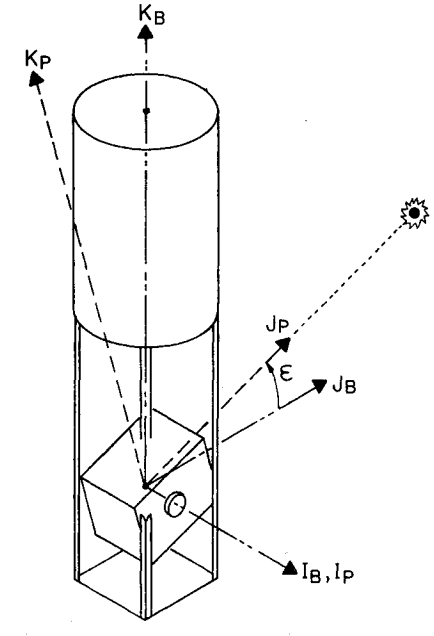

I_P, J_P, K_P = PLATFORM REFERENCE FRAME
I_B, J_B, K_B = BODY REFERENCE FRAME

Fig. 7 Payload and gimbal reference frames.

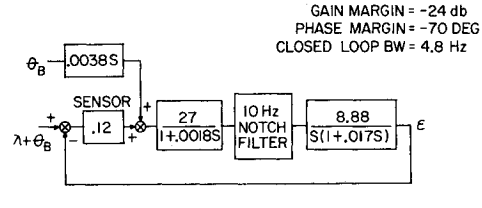

Fig. 8 Pitch servoloop.

than ±2 deg and the average roll error was well within the ±7 deg comprehensive success criteria with only momentary excursions exceeding this limit when a high-amplitude 1.5 Hz disturbance was induced. The above performance was recorded with a sun angle of 50 deg with a worst-case coning angle of 15 deg.

Flight Performance

NASA Rocket 30.006GU was launched on Sept. 15, 1980 from the White Sands Missile Range, New Mexico. All experiment objectives and mission success criteria were met on this first use of the parachute-suspended solar pointing system.[4]

Soon after payload separation, the yo-yo was deployed reducing the initial rocket spin rate of 3 to 0.125 rps. The control system was enabled at $T+155.7$ s after canopy inflation. Coarse solar acquitition was established at $T+163.6$ s, and the final pointing phase was attained at $T+170$ s at an altitude of 61 km. The altitude at this time was 34 km. At $T+771$ s, the experiment was stowed in an upright position in preparation for recovery.

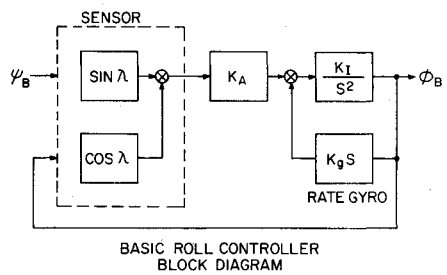

Fig. 9 Basic roll controller block diagram.

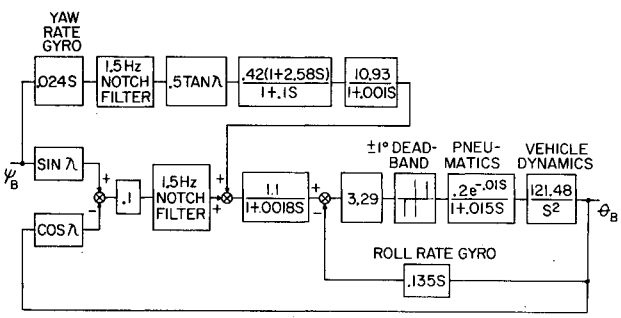

Fig. 10 Roll control loop.

The 125-lb payload exhibited a pendulous irregular coning motion during the flight with characteristic high and low frequencies of 1.56 and 0.2 Hz, respectively. The relative half-angle amplitudes of the pitch and yaw motion were deduced from rate gyro data and are shown in Figs. 11 and 12.

Typical pitch and yaw pointing errors from telemetry recordings of the gimbal-mounted MASS are shown in Fig. 13. These particular segments are in the altitude range of 50 km. The pitch error remained within ±2 deg for the entire flight. The waveform exhibits the 10 Hz belt resonance and

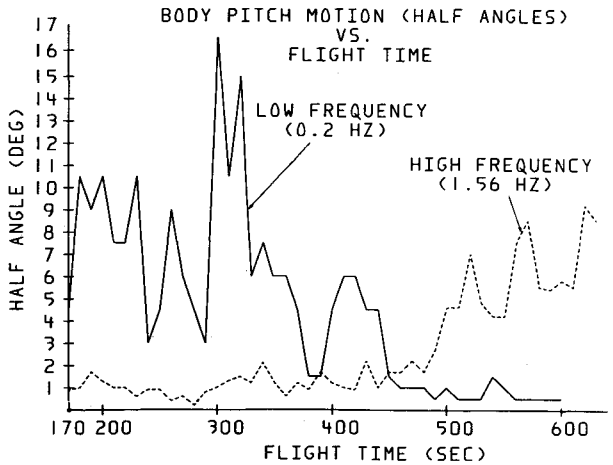

Fig. 11 Body pitch motion (half-angles) vs flight time.

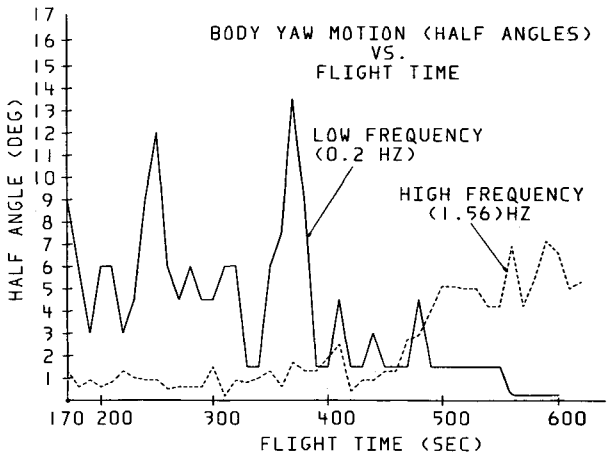

Fig. 12 Body yaw motion (half-angles) vs flight time.

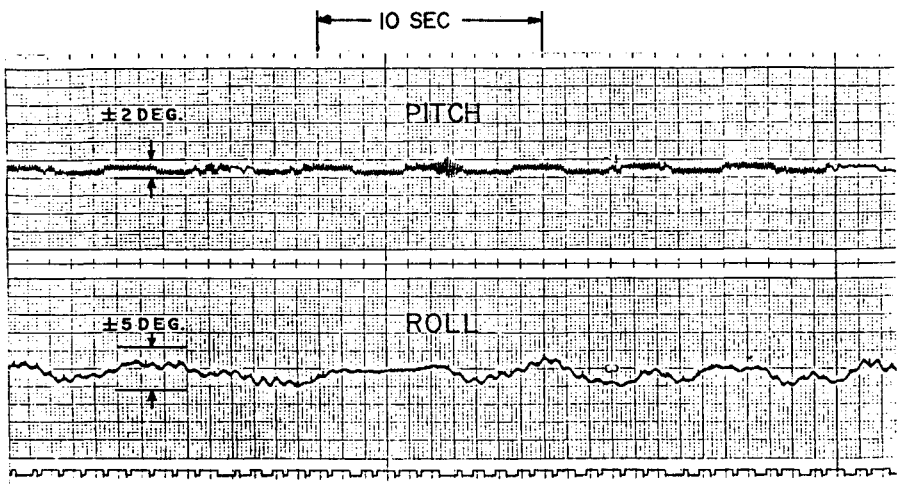

Fig. 13 Typical pitch and yaw pointing error.

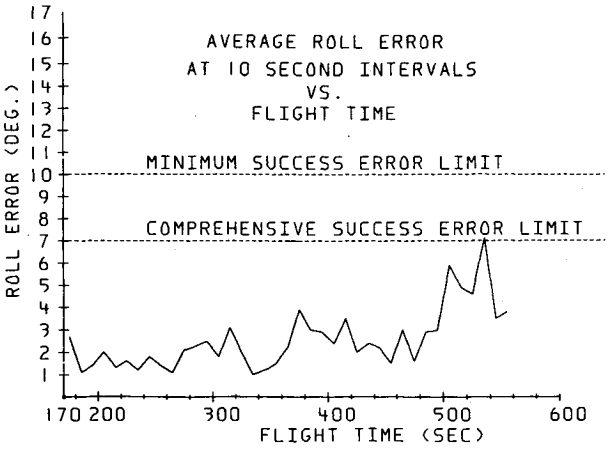

Fig. 14 Average roll error at 10-s intervals vs flight time.

also a step function due to blacklash in the gear motor. The 1.5 Hz frequency payload motion is evidenced in the roll error waveform. The average roll error plotted in Fig. 14 is within the comprehensive mission success requirements.

Conclusion

The development of the parachute-suspended solar pointing system provides a new vehicle for solar measurements in the altitude range 30 to 70 km. In the initial development, some compromises were made in the roll control loop due to restrictions on propellant storage. This resulted in increased pointing error since the 1.5 Hz disturbance could not be controlled. This has been corrected in a subsequent system which was configured with a two-axis gimbal with directive-drive torquer motors. The direct-drive mechanism eliminates the backlash and resonance problems observed in the belt drive servo system. The torquer motors were also selected to correct disturbances up to 10-deg half-angle amplitude at the 1.5 Hz frequency. All ground test data of the new system indicate that the design goals have been met. The pointing error recorded with a crane-suspended payload indicated a pointing error of less than ±0.5 deg for for sun angles up to 55 deg.

Acknowledgments

The new system described in this paper resulted from the efforts and contributions of both NASA and Lockheed SPARCS personnel. Particular acknowledgment is given to the Special Payloads Division and the Guidance and Control Branch of NASA Goddard Space Flight Center. Many long hours were spent on the analog computer simulation in support of the Lockheed work by Jim Donohue, John Celmer, and Fred Hager. Acknowledgment is also given to Louie Yamanishi and Hank Galla of the Lockheed SPARCS Project for their contributions in the fabrication and test of the payload and control system.

References

[1]Maksimovic, V., "A Parachute System for Upper Atmospheric Studies," paper presented at AIAA 5th Sounding Rocket Technology Conference, Houston, Tex. March 1979.

[2]Hansen, Q. M., Gabris, E. A., Person, M. D., and Leonard, B. S., "A Gyroless Sounding Rocket," *Journal of Spacecraft and Rockets*, Vol. 4, Nov. 1967.

[3]Hansen, Q. M., Rusk, S. J., and Gabris, E. A., "A Gyroless Sounding Rocket Control System with Sub Arc-Second Pointing Stability," *Automatica*, Vol. 6, 1970.

[4]Mentall, J. E., Frederick, J. E., and Herman, J. R., "The Solar Irradiance from 200 to 300 MM," *Journal of Geophysical Research*, Vol.86, No. C10, Oct. 20, 1981, pp. 9881-9884.

New Publication Charge Policy

Authors of manuscripts accepted for publication on or after April 1, 1984, will be requested to pay a flat-fee publication charge in lieu of the current charge of $110 per printed page. As is our present policy, *every* author's company or institution is expected to pay the publication charge *if it can afford to do so.*

Authors of U.S. Government-sponsored research, please note: Payment of such charges is authorized as a cost item in government contracts under a policy ruling by the Federal Council of Science and Technology. Under the policy, which is standard for all government agencies, charges for publication of research results in scientific journals will be budgeted for and paid as a necessary part of research costs under Federal grants and contracts. The policy recognizes that the results of government-sponsored research frequently are published in journals which do not carry advertising and which are published by nonprofit organizations (such as AIAA).

The new schedule of publication charges is as follows:

Full-length article	$750
Technical or Engineering Note	$300
Synoptic	$200
Technical Comment or Readers' Forum	$200
Reply to Comment	no charge

Payment of the publication charge entitles the author to 100 complimentary reprints.

Beginning in April, every author *not* employed by the U.S. Government will receive an invoice with his or her acceptance letter. Government-employed authors will be asked to submit a purchase order and will be invoiced upon receipt of that purchase order by AIAA.

We ask the cooperation and support of authors and their employers in our continuing efforts to disseminate the results of scientific and engineering research and development.